Beamforming Array Design and Simulation using MATLAB

Dimitrios Karatis 10775, *Electrical and Computer Engineering, AUTH*

***Abstract*—This project investigates the design and simulation of beamforming systems using both radio frequency (RF) and optical uniform linear arrays (ULAs) implemented in MATLAB. The study aims to evaluate the impact of beam steering angle, element spacing, array size, and excitation profile on the resulting radiation patterns.**

***Index Terms*—Beamforming, antenna arrays, optical phased arrays, MATLAB, linear array, radiation pattern, array factor, binomial distribution, phase shift.**

I. Introduction

This assignment explores beamforming concepts through the simulation of uniform linear antenna arrays (ULAs) in both radio and optical frequencies using MATLAB. The project is divided into two main parts.

In the first part, we focus on a classical 7-element ULA with inter-element spacing $d = \lambda/2$, operating at a carrier frequency of $f = 1\,\mathrm{GHz}$. The MATLAB code calculates the array factor and near-field distribution, enabling analysis of the beam's angular direction and shape. Simulations are conducted for different steering angles and spacing values ($d = \lambda/2$ and $d = \lambda/4$), followed by a study on arrays with 5 and 9 elements. A binomial amplitude taper is also applied to assess its effect on sidelobe reduction.

In the second part, the study extends to the simulation of an 8-element optical phased array (OPA) beamforming network at $\lambda = 1550\,\mathrm{nm}$. Phase shifts provided from experimental measurements are used to steer the beam toward specific angles ($0°$, $30°$, $60°$, and $90°$). The resulting radiation patterns are analyzed and compared to theoretical expectations based on the array factor equation.

PROBLEM 1

I. Part A: Beam Steering for Multiple Angles

A. Implementation and Theoretical Analysis

The goal of Part A is to analyze the beam steering capabilities of a 7-element uniform linear array (ULA) by simulating the field distribution and array factor for different beam tilt angles and inter-element spacings. The implementation is based on a time-harmonic excitation at $f = 1\,\mathrm{GHz}$, corresponding to a wavelength of $\lambda = 0.3\,\mathrm{m}$.

The simulation begins by defining the necessary physical constants such as the speed of light, angular frequency, and wavenumber. The observation space is discretized both radially and angularly to evaluate the 2D radiation field over a circular region. Two different element spacings are considered: $d = \lambda/2$ and $d = \lambda/4$.

For each spacing, four beam tilt angles are simulated: $\theta_0 = 0°, 30°, 60°$, and $90°$. The tilt is achieved by introducing a progressive phase shift $\delta = -kd\sin(\theta_0)$ across the elements of the array. Each element is modeled as a point source located along the x-axis, symmetrically centered around the origin. The total field at each point in space is computed by superimposing the time-harmonic contributions from all antenna elements with their respective phase shifts. A single snapshot in time is considered to visualize the spatial field distribution $E(x, y)$.

Simultaneously, the array factor (AF) is calculated analytically for each case by summing the contributions of all elements assuming uniform amplitude excitation. The AF expression used is:

$$AF(\theta) = \left| \sum_{n=0}^{N-1} |a_n| e^{j(knd\cos\theta + n\delta)} \right|$$

$$\delta = -k \cdot d \cdot sin(\theta_0), \quad |a_n| = 1$$

This term describes the far-field radiation pattern of the array normalized to its maximum. By comparing the AF plots and full field distributions across the different scenarios, we observe how tilting the beam modifies the direction of maximum radiation, and how changing the inter-element spacing affects side lobe behavior and directivity.

Detailed code for this part of the assignment can be found in the exercise1_a.m file.

B. Plot Results

Results show that halving the spacing from $\lambda/2$ to $\lambda/4$ significantly suppresses side lobes, offering better beam shaping at the cost of increased coupling.

For $\theta_0 = 0°$: When $d = \lambda/2$, the main lobe is sharply focused in the broadside direction, and several side lobes are visible, indicating high directivity but potential interference from other directions. When the spacing is reduced to $d = \lambda/4$, the pattern becomes more concentrated around the broadside with significantly lower side lobe levels. The beam remains centered but exhibits a wider main lobe.

For $\theta_0 = 30°$: With $d = \lambda/2$, the main beam steers correctly toward $30°$, maintaining a relatively narrow width. However, moderate side lobes are present. For $d = \lambda/4$, the beam is again correctly steered but now appears wider, with side lobes

This document was prepared by Dimitrios Karatis as part of the second assignment for the Advanced Antennas course at Aristotle University of Thessaloniki.

much less pronounced. The overall shape of the pattern is smoother and more compact.

For $\theta_0 = 60°$: At $d = \lambda/2$, the main lobe is still directed toward the desired angle but the pattern becomes more asymmetric, and side lobes increase in prominence, resulting in a more complex beam shape. When the spacing is decreased to $d = \lambda/4$, the pattern becomes more rounded and less distorted, with reduced side lobes and a broader, more uniform main lobe. This change indicates improved beam quality and reduced interference.

For $\theta_0 = 90°$: In the $d = \lambda/2$ case, the beam is steered toward the correct direction, producing a symmetric "infinity" pattern with moderate side lobes. When $d = \lambda/4$, the pattern becomes more rounded, with reduced side lobes and a broader main lobe.

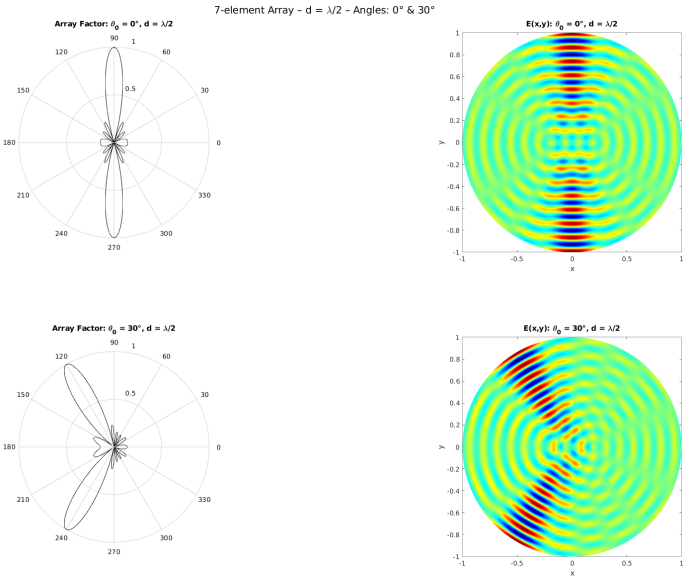

Fig. 1: Results for $d = \lambda/2$, 0 and 30 degree angles

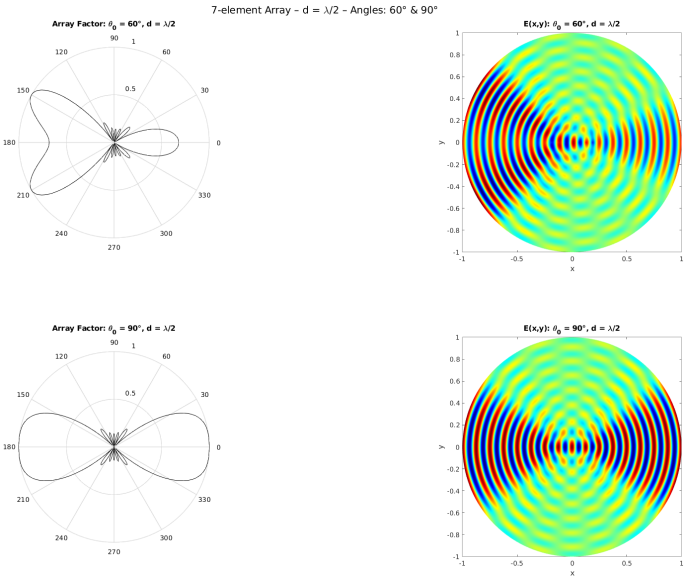

Fig. 2: Results for $d = \lambda/2$, 60 and 90 degree angles

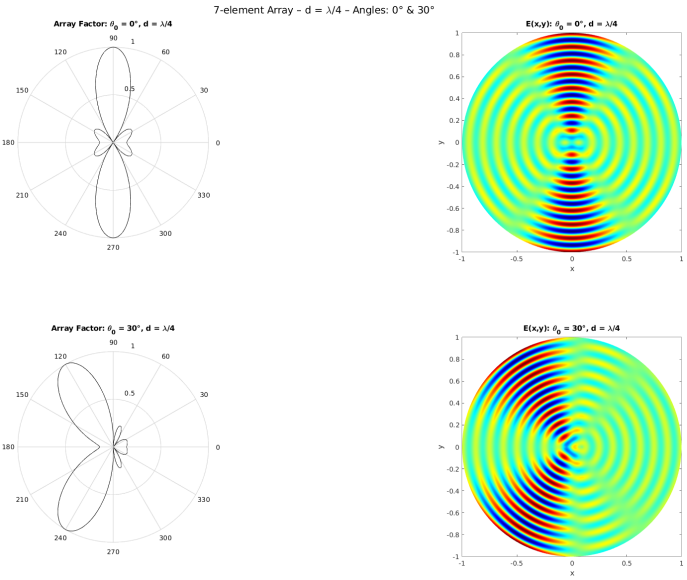

Fig. 3: Results for $d = \lambda/4$, 0 and 30 degree angles

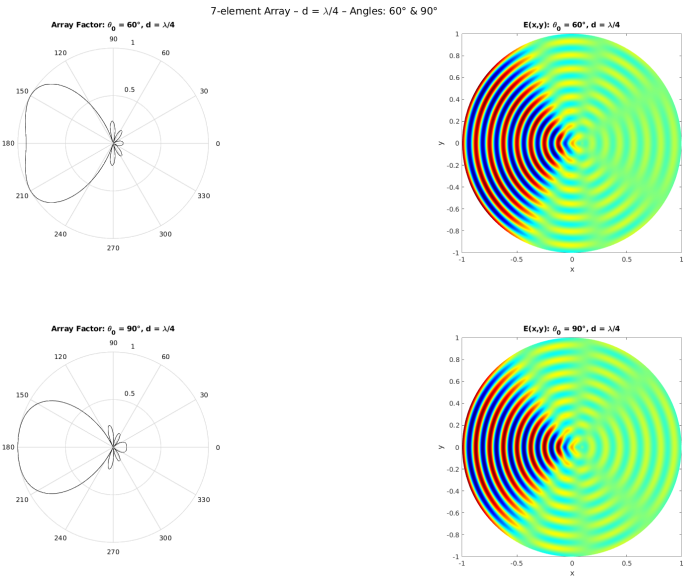

Fig. 4: Results for $d = \lambda/4$, 60 and 90 degree angles

II. Part B: Varying the Number of Elements

A. Implementation and Theoretical Analysis

To study the impact of array size, the MATLAB script is modified to simulate ULAs consisting of 5 and 9 elements, respectively. In both cases, the spacing remains $d = \lambda/2$, and the operating frequency is fixed at 1 GHz. The goal is to observe how the size of the array affects the directivity, beamwidth, and sidelobe structure for different steering angles.

The code begins by defining the physical and simulation parameters, such as the operating frequency $f = 1\,\text{GHz}$, wavelength $\lambda = c/f$, and the discretization for the observation domain. The radiation field is evaluated over a polar grid spanning a distance from 0 to 8λ and an angular range of $0°$ to $360°$, discretized into 240 angular samples.

The array geometry is constructed such that the antenna

elements are symmetrically placed around the origin along the x-axis. For each array size ($N = 5$ and $N = 9$), the excitation coefficients are kept uniform, and a phase shift $\delta = -kd\sin(\theta_0)$ is applied to steer the beam toward angles $\theta_0 = 30°$ and $90°$. At a fixed time instant, the radiated field $E(x, y)$ is computed by summing the individual contributions of each element, taking into account both phase and spatial delay.

Additionally, the array factor is computed analytically using the standard formulation for a ULA:

$$AF(\theta) = \left| \sum_{n=0}^{N-1} e^{j(knd\cos(\theta)+n\delta)} \right|, \quad \delta = -k \cdot d \cdot sin(\theta_0)$$

Detailed code for this part of the assignment can be found in the exercise1_b.m file.

B. Plot Results

The simulation results include both the normalized array factor plotted in polar form and the spatial distribution of the field intensity. These visualizations clearly demonstrate that increasing the number of elements leads to a narrower main lobe and improved directivity. Furthermore, the sidelobe levels are reduced, making the array more capable of suppressing unwanted radiation in undesired directions. The results highlight the importance of array size in achieving sharper and more controllable beam patterns.

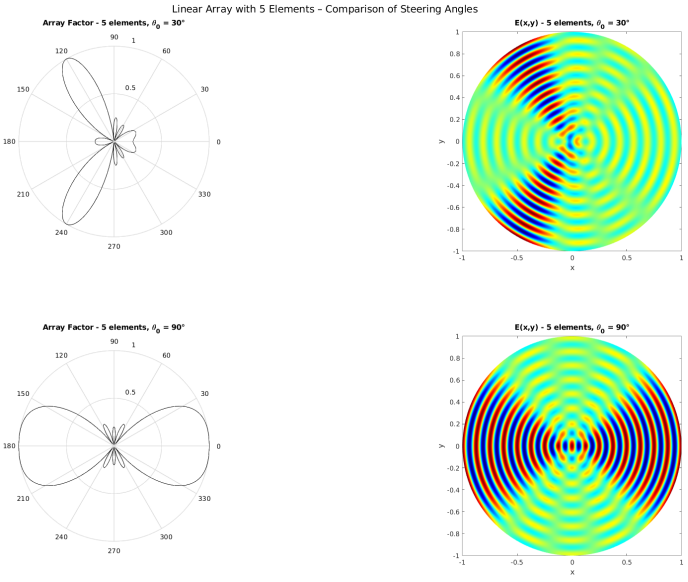

Fig. 5: Results for 5 elements

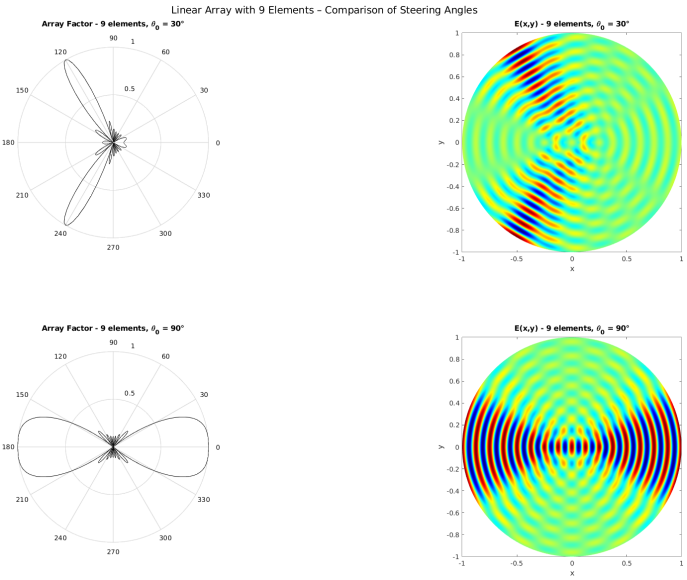

Fig. 6: Results for 9 elements

III. Part C: Binomial Amplitude Distribution

A. Implementation and Theoretical Analysis

In this final part of the simulation, a linear antenna array of $N = 7$ isotropic elements is analyzed under a non-uniform amplitude excitation. Specifically, the elements are weighted using a binomial distribution, which is known to suppress side lobes at the cost of widening the main lobe and enhance the overall radiation pattern quality. This configuration is compared against the previously used uniform weighting in terms of sidelobe levels and main lobe shape.

The system maintains a half-wavelength element spacing of $d = \lambda/2$, with the beam steered toward $\theta_0 = 30°$. The binomial weights are computed using the binomial coefficient:

$$A_n = \binom{N-1}{n}, \quad n = 0, 1, \ldots, N-1$$

These coefficients are normalized so that the maximum amplitude is unity.

As in previous exercises, the array is centered along the x-axis, with the element positions symmetrically distributed about the origin. The total radiated field $E(x, y)$ is calculated by summing the individual contributions from each element:

$$E(x, y) = \sum_{n=0}^{N-1} A_n \cos\left(\omega t - kR_n + \delta(n - \tfrac{N-1}{2})\right)$$

where R_n is the distance from the n-th element to each observation point and $\delta = -kd\sin(\theta_0)$ is the progressive phase shift used to steer the main lobe.

Additionally, the theoretical array factor (AF) is calculated using the analytical expression:

$$AF(\theta) = \left| \sum_{n=0}^{N-1} A_n e^{j(knd\cos(\theta)-n\delta)} \right|$$

Detailed code for this part of the assignment can be found in the exercise1_c.m file.

B. Plot Results

The simulation output includes both the polar plot of the normalized array factor and a spatial representation of the total field $E(x, y)$. The application of binomial weighting significantly alters the characteristics of the beam pattern. Specifically, it suppresses the side lobes almost entirely. This is evident in the polar plot of the array factor, where the radiation pattern becomes much smoother and the side lobes are drastically reduced compared to the previous cases. However, this improvement in side lobe suppression comes at the cost of main lobe broadening and a reduction in directivity.

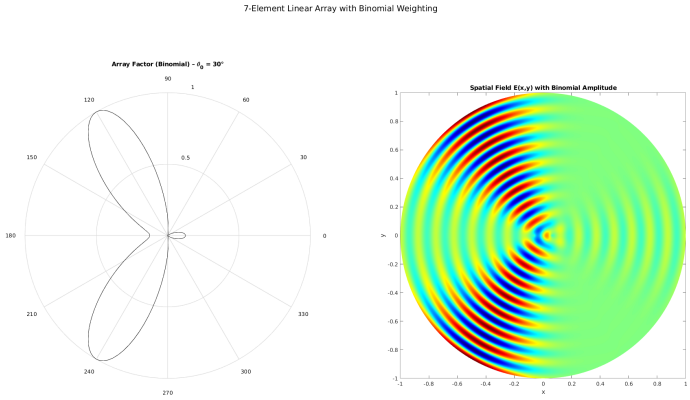

Fig. 7: Results for Binomial Weighting

CONCLUSION

All in all,this exercise investigated the radiation behavior of linear antenna arrays under different design conditions. In Part 1a, beam steering was achieved using uniform excitation and varying steering angles and spacings, demonstrating how phase shifts control beam direction. Part 1b compared arrays of different sizes, confirming that more elements yield narrower main lobes and improved directivity. In Part 1c, binomial amplitude weighting was applied to reduce sidelobe levels, at the cost of broader main lobes. Overall, the simulations illustrated key trade-offs between directivity, sidelobe suppression, and array complexity in antenna design.

PROBLEM 2

I. PART A: OPTICAL BEAM STEERING WITH PHASE SHIFTER CONFIGURATION

In this simulation, we aim to demonstrate that the phase values given in Table 1 of the assignment correctly steer the beam of a linear optical phased array consisting of 8 radiating elements at angles of 0°, 30°, 60°, and 90°. The implementation follows the simulation logic and methodology presented in Exercise 1, adapted to the optical domain with a central wavelength of 1550 nm.

System Configuration

The optical phased array (OPA) under consideration consists of $N = 8$ isotropic elements, uniformly spaced by a distance $d = \lambda/2$, where $\lambda = 1550$ nm is the optical wavelength. The array is assumed to be linear and centered at the origin, with the positions of the antenna elements defined as:

$$x_n = \left(n - \frac{N+1}{2}\right) \cdot d, \quad n = 1, 2, ..., 8$$

The phase shifts for each element are applied externally using dedicated phase shifters, as shown in the beamforming architecture of Table 1 in the assignment.

Input Phase Profiles

The phase values $|\phi_n|$ applied to each element for beam steering at angles $\theta_0 = 0°$, 30°, 60°, and 90° are provided in Table 1 of the assignment and are implemented directly in the simulation. These values represent the required external phase shifts (after the Mach-Zehnder interferometer) that align the interference of the optical signals in the desired direction and were obtained after real-life measurements. These values, given in radians, are listed below for the four beam steering directions $\theta_0 = 0°$, 30°, 60°, and 90°:

θ_0	Phase Values $\lvert\phi_n\rvert$ (radians)
0°	0.0, 0.0, 0.0, 0.0, 0.0, 0.0, 0.0, 0.0
30°	0.0, 2.657, 2.1724, 1.6878, 1.2032, 0.7186, 0.234, 5.5319
60°	0.0, 2.9921, 5.9842, 2.6931, 5.6852, 2.3941, 5.3862, 2.0951
90°	0.0, 1.4077, 2.8153, 4.2230, 5.6307, 0.7551, 2.1628, 3.5705

For comparison, the theoretical phase values for steering the main beam toward θ_0 are calculated using the formula:

$$\phi_n = -n \cdot k \cdot d \cdot \sin(\theta_0)$$

where:

- $k = \dfrac{2\pi}{\lambda}$ is the wavenumber,
- $d = \dfrac{\lambda}{2}$ is the inter-element spacing,
- $n = 0, 1, ..., 7$ (element index from the leftmost element),
- θ_0 is the desired steering angle.

The resulting theoretical phase values (in radians) are:

θ_0	Theoretical Phase Values $\lvert\phi_n\rvert$ (radians)
0°	0, 0, 0, 0, 0, 0, 0, 0
30°	0, 1.57, 3.141, 4.712, 6.283, 7.854, 9.424, 10.995
60°	0, 2.720, 5.441, 8.162, 10.882, 13.603, 16.324, 19.044
90°	0, 3.141, 6.283, 9.424, 12.566, 15.708, 18.849, 21.991

Comparing the empirical and theoretical values reveals significant differences. While the theoretical model assumes ideal phase shifts derived from the array geometry, the values in Table 1 are much different.

Simulation Methodology

The array factor (AF) is computed for each steering angle by summing the contributions of each element across the domain. The mathematical formulation used is:

$$AF(\theta) = \left| \sum_{n=1}^{N} |a_n| e^{[j(nkd_x \sin(\theta) - |\phi_n|)]} \right|$$

$$|a_n| = 1$$

where:

- $k = \dfrac{2\pi}{\lambda}$ is the optical wavenumber,
- d_x is the position of the n and $n-1$-th element,
- ϕ_n is the applied phase shift for steering the beam.

The array factor is evaluated over a full $360°$ angular range and normalized with respect to its maximum value for each case. The resulting radiation patterns are plotted in polar form to visualize the direction and shape of the main beam.

Detailed code for this part of the assignment can be found in the exercise2_a.m file.

Results and Interpretation

The following polar plots show the normalized array factor (AF) for an optical phased array with 8 elements spaced at $d = \lambda/2$, operating at a wavelength $\lambda = 1550\,\text{nm}$. The excitation phases are taken from real measurements (given in the assignment) corresponding to the four steering directions.

- **At** $\theta_0 = 0°$: The excitation phases are all zero, resulting in a symmetric beam pattern centered at $0°$ (broadside). This confirms correct beam formation along the desired direction.
- **At** $\theta_0 = 30°$: The main beam appears steered approximately toward $15°$, which is significantly less than the intended direction. Additionally, the side lobe levels are noticeably elevated. This suggests that the applied phase profile does not perfectly match the theoretical requirement for steering to $30°$.
- **At** $\theta_0 = 60°$: The beam pattern deviates drastically from expectation. Instead of steering toward $60°$, the main lobes appear around $90°$ and $270°$, forming a pattern resembling the shape of an "infinity" symbol. Again, the beam does not match with the intented one.
- **At** $\theta_0 = 90°$: The main beam is steered incorrectly toward approximately $-30°$, which is inconsistent with the desired radiation at $90°$. Again, it doesn't seem that the beam matches the intented one.

These results highlight that the measured phase profiles deviate from the theoretical formula:

$$\phi_n = -nkd\sin(\theta_0)$$

where n is the element index and $k = 2\pi/\lambda$ is the optical wavenumber. In theory, this ensures beam maximum at $\theta = \theta_0$. However, the measured phase sets provided (possibly affected by hardware nonlinearities, Mach-Zehnder interferometer imbalance, or quantization) introduce unintended shifts and distortions.

Conclusion

The results demonstrate that although the array is capable of forming and steering a beam, the actual steering direction deviates significantly from the intended one when measured (non-ideal) phase values are used. These errors become more pronounced at higher steering angles, especially at $\theta_0 = 60°$ and $90°$, where the beam is either highly distorted or misdirected. This underscores the sensitivity of optical phased arrays to precise phase control.

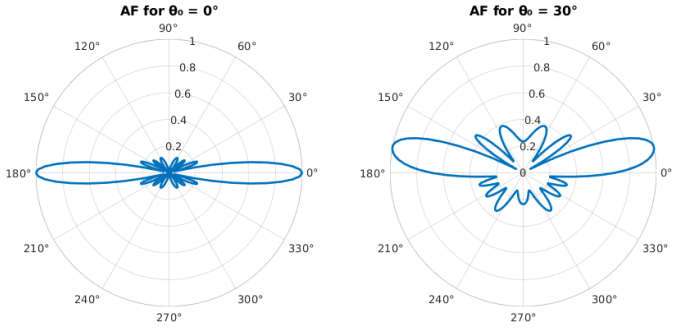

Fig. 8: AF for 0°, 30° when using $|\phi_n|$ from Table 1

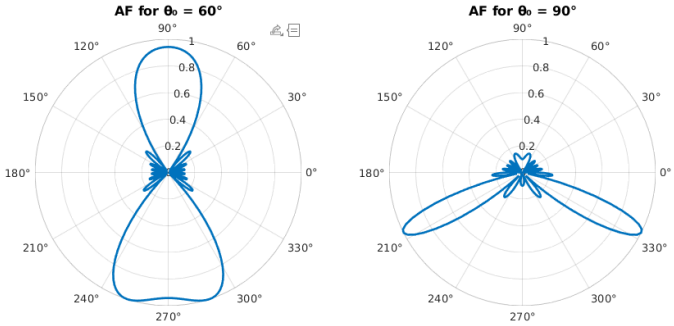

Fig. 9: AF for 60°, 90° when using $|\phi_n|$ from Table 1

II. PART B: BINOMIAL AMPLITUDE DISTRIBUTION IN OPTICAL PHASED ARRAYS (OPA)

The binomial distribution derives its amplitude weights from the coefficients of a binomial expansion:

$$(1+x)^{N-1} = \sum_{n=0}^{N-1} \binom{N-1}{n} x^n$$

For a linear array of N elements, the coefficients $\binom{N-1}{n}$ are used to define the relative amplitude $|a_n|$ of each element. These values are typically normalized to ensure that the total radiated power remains within desired limits.

This amplitude tapering profile is known to:

- Minimize or completely eliminate side lobes in the radiation pattern,
- Slightly widen the main lobe as a trade-off for higher beam purity,
- Improve angular discrimination in high-precision optical applications.

Qualitative Procedure to Apply the Distribution

To apply binomial amplitude distribution in an OPA:

1) **Determine the number of array elements** N. This defines the order of the binomial expansion.
2) **Compute the binomial coefficients**:
$$[|a_1|, |a_2|, \ldots, |a_N|] = \left[\binom{N-1}{0}, \binom{N-1}{1}, \ldots, \binom{N-1}{N-1}\right]$$
3) **Normalize the amplitudes** so that either the peak value is 1 or the sum of all weights equals 1.
4) **Assign the normalized amplitude values to the excitation signals of each element**.
5) **Simultaneously apply phase shifts** (using phase shifters) to steer the beam toward the desired angle θ_0 as per:
$$\phi_n = -nkd_x \sin\theta_0$$
where $k = \frac{2\pi}{\lambda}$ and d_x is the spacing between adjacent elements.

Practical Implementation in Optical Systems

Figure 1 in the assignment illustrates the optical beamforming architecture used to distribute and modulate optical signals across the antenna elements. Each node in the optical routing network is referred to as an **Xbar node**, which includes:

- A **Mach-Zehnder Interferometer (MZI)** — used to control the **amplitude** of the signal.
- A **phase shifter (PS)** — used to control the **phase** of the signal.

As shown in Figure 2 of the assignment, the Mach-Zehnder Interferometer consists of two optical arms with a path length difference ΔL. By applying a phase shift to one of the arms, the optical interference at the output changes, which in turn modifies the amplitude of the signal exiting the MZI. This is the key mechanism through which binomial amplitude values can be implemented optically.

The mathematical expression describing the output electric fields from the MZI is given in the assignment as:

$$\begin{bmatrix} E_{01}(f) \\ E_{02}(f) \end{bmatrix} = e^{-j\beta(2l+L)} \begin{bmatrix} \frac{1}{\sqrt{2}} & \frac{j}{\sqrt{2}} \\ \frac{j}{\sqrt{2}} & \frac{1}{\sqrt{2}} \end{bmatrix} \begin{bmatrix} 1 & 0 \\ 0 & e^{j\beta\Delta L} \end{bmatrix} \begin{bmatrix} \frac{1}{\sqrt{2}} & \frac{j}{\sqrt{2}} \\ \frac{j}{\sqrt{2}} & \frac{1}{\sqrt{2}} \end{bmatrix} \begin{bmatrix} E_{i1}(f) \\ E_{i2}(f) \end{bmatrix}$$

From this expression, it is evident that the output amplitudes are directly influenced by the phase difference ΔL applied within the interferometer. Therefore, by carefully tuning ΔL in each MZI, the amplitude of the signal feeding each antenna element can be shaped to match the desired binomial weight.

Conclusion

The binomial amplitude distribution can be effectively applied in an optical phased array system to suppress side lobes and improve radiation directivity. By leveraging the functionality of Mach-Zehnder Interferometers for amplitude control (as shown in Figures 1 and 2), and external phase shifters for directional beam steering, a fully controlled amplitude and phase profile can be achieved.